Drug Delivery System

VOL.23 NO.1 JANUARY 2008

通巻第 117 号／隔月刊

Offprint

Title

Name

Department

Institution

Address

Postal Code City Country

Phone Fax

The Japan Society of Drug Delivery System

Institute of Medical Science
St. Marianna University School of Medicine,
Sugao, Miyamae-ku, Kawasaki, Kanagawa Pref, 216-8512 JAPAN

ターゲティングを用いたMRI造影剤

特集　分子イメージングとDDS

白石貢一・横山昌幸*

MRI contrast agents with targeting ability

In recent several years, the drug targeting methodology has been actively applied to MRI contrast agents, particularly to "selective MRI contrast agents" that can only enhance image contrasts at target sites. This situation is one part of reflection of fusion between DDS and molecular imaging fields. This review describes how and for what purpose drug targeting can be applied to developments of novel MRI contrast agents. This review is composed of the following contents : concept of selective MRI contrast agents, methodological differences between the targetings of drugs and contrast agents, mechanisms of selective contrasts, and the authors' study of polymeric micelle MRI contrast agents.

MRI造影剤，特に対象部位のみを選択的に画像化できる造影剤に，ターゲティング研究の成果が積極的に用いられはじめている．この状況は，DDSと分子イメージングが融合する領域で，今後の大きな発展が期待される．本総説は，DDS側からみてこの融合領域にどのようにアプローチしうるかについて，筆者らの研究例を盛り込んで解説した．具体的には，選択的MRI造影剤の概念，薬物と造影剤の場合のターゲティングの相違点，造影剤で選択性を得る方法，高分子ミセルキャリアを用いた造影剤の研究例である．

*Kouichi Shiraishi · Masayuki Yokoyama**

key words : targeting, MRI, contrast agent, molecular imaging, diagnosis

ターゲティングを用いた選択的造影剤

造影剤とは，観察したい対象の画像コントラストを高めてより見やすく，診断しやすい画像を得るために投与される化合物である．最も単純な造影剤の使われ方は，X線の血管造影剤が代表例である．カテーテルによって導かれた部位に造影剤を注入し，その部位の血流を造影剤の高いX線吸収能によって可視化する．この場合，造影剤の生体内動態・分布の要素はまったく問題にならず，投与部位から速やかに近傍に拡散すればよいのである．

一方，少数ではあるが造影剤が投与されたあとに特定の所に集積する，あるいは集積しないことを通して，特定の部位のみを選択的に可視化する場合がある．後述する脳腫瘍診断で用いるMRI造影剤がこの例である．

本総説では，このようなターゲティングを用いた選択的造影剤をMRIに焦点を当てて，DDSターゲティング技術との関連を述べる．

まずここで強調しておきたいことは，DDSと造影剤は歴史的にはまったく別個といってもよい発展の道をたどってきたことである．後述する低分子のMRI造影剤はGdイオンのキレート化合物で，その設計の鍵は配位定数(いかにGdイオンをしっかりと結合するか)と化合物の荷電による体内での浸透圧調節であった．この設計にはDDS的な観点は存在しない．

一方，DDSのターゲティング研究でも，体内分布測定のための画像を撮ることはあっても，それをMRI診断までに実用化しようとする研究は1990年代まではほとんどなかった．デキストラン[1]，アルブミン[2]，リポソーム[3]にキレート化合物を結合・内封させることによる高分子型のMRI造影剤研究がわずかに行われていたにすぎない．1990年代になり，DDSを応用したMRI造影剤研究数の増加を

* Yokoyama "Nano-medical polymer" project, Kanagawa Academy of Science and Technology　神奈川科学技術アカデミー横山「高分子ナノメディカル」プロジェクト

表1　選択的MRI造影剤の種類

造影剤の種類	造影剤	キャリア	ターゲット/作用
T_1強調型	MS-325	アルブミン	アルブミンとの結合
	EGad	なし	β-ガラクトキシダーゼ
	Gd-*bis*-5-HT-DTPA	なし	ミエロペルオキシダーゼ
	MPEG-PL-Gd-DTPA	Poly(L-lysine)-PEG	EPR効果
T_2強調型	cRGD-CLIO(Cy5.5)	デキストランコーティング	$\alpha_v\beta_3$インテグリン
	MnMEIO-herceptin	デキストランコーティング	HER2

みたが，わずかなものにとどまっていた．

この状況が一変するのは，最近5年ぐらいの“分子イメージング”研究開発の急速な発展である．分子イメージングとは「特定の細胞・組織・臓器が産生する分子，あるいはその分子によって誘起された現象を画像化すること」と定義される．一方，ターゲティングが「特定の細胞・組織・臓器に薬物を選択的に運搬して働かせること」であるので，原理的な類似性は明白である．リポソームや高分子ミセルキャリアによる抗がん剤の臨床試験が盛んになってきた2000年代のターゲティングの状況と分子イメージング研究の勃興が時代的に重なり合っている現在が，まさに選択的MRI造影剤を推し進める好機であると考えられる．

ただし，この好機を有効に活用にするためには，薬物のターゲティングと造影剤のターゲティングとの間の相違点を正確に把握することが重要である，と筆者らは考えている．その相違点として考えられるのはつぎの3点であり，以下に具体例として抗がん剤のターゲティングとの比較を述べる．

1. 送達する量の問題

この量の側面には二つある．まず第1に，Gdイオンを利用した造影剤はかなり投与量が多いことである．代表的なMRI造影剤のMagnevistの標準投与量は55 mg/kg(最大は165 mg/kg)とかなり多い(抗がん剤の投与量は臨床では体表面積(mg/m^2)であらわされることが多いので比較には注意が必要である)．抗がん剤にくらべると5～50倍くらい大きな投与量である．これくらい投与量が大きいとキャリア自体の量も問題となる．投与に必要なキャリアの量が膨大になり，その高い粘度によってマウスへの投与時に問題がある例が散見される[4]．

量に関する第2の点は，造影剤の場合には標的に到達させるべき割合に具体的な目標値が設定できない場合がある．抗がん剤のターゲティングの場合には，投与量のうちどれくらいの割合ががんに送達されないとターゲティング効果が発揮されないという最低割合が存在する．がん以外の正常部位に到達したものは副作用を起こすので，がんへ到達する割合を高めることが重要なのである．造影剤の場合には，造影に必要な絶対量(投与量に対する割合でなく)が送達され，そのときに標的と見分けるべき部位の送達量が充分に低ければよい．この見分けるべき部位が血管(血液)である場合には，抗がん剤の場合の正常組織・臓器への分布は無視できることとなる．

2. キャリア設計

抗がん剤ターゲティングでは，キャリアの選択のみならず，抗がん剤とキャリアの重量比がターゲティング性能を決める重要な因子であることが広く認識されている．

しかし，これまでのMRI造影剤研究では，たんにキャリアに結合さえすればキャリアの性能を100%引き出せるという仮定に基づいて行われた研究が多く，造影剤構成比がその物理化学的性質の変化を通して体内動態・分布に及ぼす影響を検討した研究はほとんどない(モノクロナール抗体が実用的に得られるようになった1980年代に，抗がん剤を抗体に結合さえすれば必ずターゲティング効果が発揮されると信じられたことと類似する)．この側面からも，現時点でDDSターゲティング技術が造影剤技術に寄与できることが多いと筆者らは信じている．

3. 毒　性

治療と診断では許容される危険度が大きく異なる

のは自明なことである．抗がん剤治療ではかなり重篤な副作用の出現も，ある範囲内であれば許容されうるが，対象ががんであっても，診断では重篤な副作用は限りなくゼロに近づけることが求められる．

よって，キャリア自体の毒性も抗がん剤ターゲティングでは問題にならないレベルでも，MRI造影剤を対象とした場合には大きな問題となることがありうる．したがって，キャリア研究においても抗がん剤ターゲティングで得られた情報を生かしつつも，より広範な副作用解析が求められる．

MRI造影剤の原理と種類

MRI造影剤にはT_1強調型とT_2強調型の大きく二つに分けることが出来る(**表1**)．T_1は縦緩和時間，T_2は横緩和時間とよばれ，どちらも造影剤近傍に存在する水分子のH(プロトン)のT_1，T_2緩和時間を短くしてMRIの信号強度に影響を及ぼすパラメーターである．それぞれのT_1，またはT_2緩和時間を短くし，画像を強調する能力はT_1緩和能またはT_2緩和能という値で数値化されている．

T_1強調型MRI造影剤は陽性造影剤とよばれ画像上を白くあらわす造影剤であるのに対して，T_2強調型MRI造影剤は画像上において黒く表現する陰性造影剤とよばれる．T_1強調型のMRI造影剤は，主にGdイオンを有する錯体化合物からなっている．Gdイオン自身は毒性が高く，そのままでは用いることは出来ないが，キレート化剤を用いて錯体化することによってその毒性を無毒化している．こういったキレート化剤の一部を高分子鎖に結合させると高分子型のMRI造影剤となる．

1. 低分子の選択的MRI造影剤

Gd-DTPA(マグネビスト)やGd-DOTA(マグネスコープ)は，全体として負のイオン性を有している(DTPAとDOTAはキレート化合物の種類を示す)．キレート化剤DOTAの四つのカルボキシル基のうち一つを変えたGd-HP-DO3A(プロハンス)は非イオン性のMRI造影剤であり，浸透圧が低く高投与量が可能となる．これらの造影剤は，静脈内投与によって血管にコントラストを与え，そして血管から容易に浸透する組織にも同様にコントラストを与える．このことを利用して脳腫瘍を選択的に造影することが出来る．脳腫瘍は血管の漏洩性が亢進しており，通常，漏れないような薬剤でも血管外へ漏出する．その結果，脳腫瘍部に造影剤が到達し，選択的に脳腫瘍を強調して造影することが出来る．

一方，Gdイオンを囲むキレート化剤に芳香族環を導入することによって上述したMRI造影剤よりも脂溶性を高めることが出来る．Gd-BOPTAやGd-EOB-BOPTAはそういった例であり，肝細胞特異的MRI造影剤として用いられている．Gd-EOB-BOPTAのような肝細胞特異性MRI造影剤は，肝臓がんのヘパトサイトの減少により肝臓がんの検出にその効果を発揮する[5]．こういった生体内の正常部位と病変部位との相違を造影剤が取り込まれる，または取り込まれないことによって造影する手法は従来から用いられてきた．

2. キャリアを用いた選択的MRI造影剤

キャリアを用いた造影剤として，まずあげられるのがT_2強調型MRI造影剤，いわゆる磁性微粒子である．磁性微粒子はそのもの自身を投与するわけではなく，SPIO(super paramagnetic iron oxide)とよばれる5～35 nmの磁性酸化鉄や，USPIO(ultrasmall super pramagnetic iron oxide)とよばれる4～6 nmの磁性酸化鉄をそれぞれデキストランで7～8 nmの厚みにコーティングした粒子として加工されている．これらのMRI造影剤は主に肝臓の細網内皮系に取り込まれ，正常な肝臓の信号強度の低下させることで特異的な可視化を可能にしている．デキストランコーティングされた磁性微粒子はキャリアを有するMRI造影剤となる．最近では，このデキストランコーティングされた磁性微粒子のサイズを自由に制御し，T_2緩和能を変化させる研究も行われている．

アミノ化CLIO(cross linked iron oxide)とよばれる磁性微粒子は，デキストランコーティングされた磁性微粒子の外側にアミノ基を有し，種々の官能基を結合させることが可能な微粒子である．このアミノ化CLIOのアミノ基の一部にcRGD部位を，残ったアミノ基に蛍光標識を導入したcRGD-CLIO

(Cy5.5)は$\alpha_v\beta_3$インテグリンをターゲットとして，腫瘍の血管新生や動脈硬化を検出するMRI造影剤として*in vivo*評価も報告もされている[6]．

延世大学のJ. Cheon教授らは，磁性微粒子の性質・サイズを自由に制御できることを報告し，*in vivo*への応用を示した．磁性微粒子は通常，一般式$MOFe_2O_3$であらわされる．Mの金属種をたとえばMn，Co，Ni，Feに変えると，その磁気モーメントが異なり，それぞれの持つT_2緩和能が異なる．また，それらの磁性微粒子は，そのサイズによっても磁気モーメントが異なり，同教授らは4 nm，6 nm，9 nm，12 nmとサイズの異なるMEIO (magnetic engineering iron oxide)とよばれる磁性微粒子を作製し，T_2緩和能が異なることを示した．この磁性微粒子にハーセプチンを結合させたMEIOは，HER2感受性のMRI造影剤となり，*in vivo*においてMnを有したMnMEIO-herceptinは，最大35%程度のT_2緩和能の変化が観察されている[7]．

T_1強調型MRI造影剤の場合は，水との相互作用がT_1短縮作用に影響を与える．一方で，Gdキレートを合成高分子や蛋白に結合すると，それ自身が高分子量化しT_1短縮作用，つまり画像コントラストをつけるためのT_1緩和能が向上する．これは高分子の運動性が低分子にくらべて落ち，水との相互作用が効率よく行われることが原因である．この第1世代といわれる高分子量化によって造影剤の感度(緩和能)を上げる試みは，いわゆる高分子型MRI造影剤(macromolecular MRI contrast agent)として，さまざまな高分子化されたMRI造影剤が合成された．

血管プール造影剤(blood pool agent)は，至適造影時間を長くすることによって血液プール相で高いコントラスト分解能と空間分解能の血管撮像を行うことが出来る．そのもの自身は低分子のGdキレートであるMS-325は，投与後に血液中のアルブミンと結合して高分子量化され，血管からの漏出しにくくなる．MS-325の高分子量化は血液中の滞留性が向上するばかりではなく，T_1緩和能が向上するという利点もある．このほかに分子量が約17,000のGadomer-17やデンドリマーを用いたMRI造影剤も同様に高分子化されることで，血中滞留性が向上するとともにT_1緩和能が高まる血管プール造影剤として報告されている．

T_1強調型MRI造影剤もキャリアを有するMRI造影剤の研究が進められている．リポソームの内水層にGdキレートを内包する手法や，Gdキレートの脂質を用いてリポソームやミセル(低分子からなるもの)を作製する．こういったリポソームやミセルの例は，外側にアクティブな抗体を結合させた例が多くみられる．

そういったなかでハーバード大学のR. Weissleder教授らは，ポリリシン鎖のアミノ基にGdキレートを部分的に導入し，残ったポリリシン鎖のアミノ基にPEG鎖を導入した分子量69万のMPEG-PL-Gd-DTPAを用いて，明確に腫瘍選択的なMRI造影剤を目的とした研究を報告した[8]．側鎖にPEG鎖を導入することでEPR効果を充分に発揮できるほどの血中滞留性を持ったMRI造影剤であった．このポリマーの分子量の大きさに対応して血中半減期が長くなり，腫瘍に充分に集めるためには分子量69万のような大きな分子量が必要となる．その反面，血中濃度が高くなり，腫瘍・血液におけるGdキレートの濃度比が小さくなってしまうことがわかっている．

3. 感度を増幅できるMRI造影剤

最近では，さらに生体内の特定の細胞・組織・臓器で引き起こされる現象を，分子・細胞レベルで無侵襲で計測し，画像化する分子イメージングが活発に研究されている．分子イメージング的手法は，日本ばかりでなく世界的にもPET(positron emmision tomography)や近赤外画像法のような測定方法が主流となり，分子イメージングの中核が形成されているといっても過言ではない．MRIは，生体内の分子分布情報をもとにして画像化する観点からすると分子イメージングに則った領域であり，さまざまな計測手段を持つMRIは，これからの将来，そのプローブ開発とともにさらなる展開が期待される．

MRIは空間分解能と解像度に利点を持つ反面，PETや近赤外画像に対して検出感度という不利な点を有する．この欠点をいかに克服していくかが

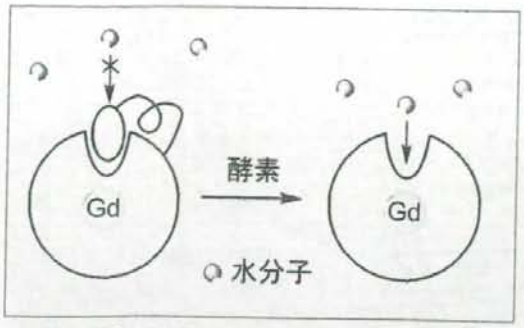

図1　酵素による化学結合切断を利用したEGad造影剤

MRI造影剤を開発する研究者にとっての課題となっている．

こうしたなかで，MRIにおける検出感度をMRI造影剤によって補うことは自然の流れのように思われる．Weissleder教授らは分子イメージングの方向性を以下のように示している[9]．

① 適切な体内動態で高い選択性を有する．
② 生体内に目的部位へのデリバリーを行える．
③ 感度を増幅できる．
④ 高感度，高速，高解像度でイメージングする．

このなかで③にあげた感度を増幅できるプローブ（造影剤）がMRIにおける欠点を補うことが出来ると考えられる．マサチューセッツ大学のA. Bogdanov教授らも同様に，MRIプローブにおける感度増幅のための戦略（amplification strategy）を提唱している[10]．

ここでは，ある特定酵素をターゲットとしてMRI造影剤の感度を向上させる“Sensitive MRI Contrast Agent”の研究例を以下にあげる．これらの研究は，病変部のバイオマーカーを主に造影剤の活性源として用いており，研究の初期段階ではあるが第2世代のMRI造影剤の例といえる．

1997年にノースイースタン大学のT. Meade教授らは，β-ガラクトキシダーゼに認識されるMRI造影剤，EGadを合成した（**図1**）[11]．この化合物EGad自身はGd-DOTAがもとになっている化合物であるが，D-ガラクトピラノーゼによって，Gdイオンへの水のアクセスが制限されており，MRI造影剤としてのT_1緩和能を充分に発揮することが

図2　酵素による酸化反応を利用したGd-*bis*-5-HT-DTPA

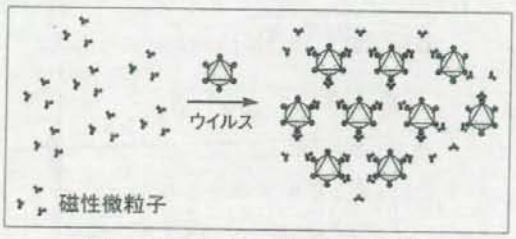

図3　ウイルスによる磁性微粒子の凝集構造

出来ない．しかしながら，β-ガラクトキシダーゼによって，このD-ガラクトピラノーゼ基が切断されると水のアクセスが容易に行われるようになり，MRI造影剤としての活性を発揮する性質を有する造影剤である．また同教授らは，Ca^{2+}やZn^{2+}よって同様に水のアクセスを制御する化合物の合成に成功している[12,13]．

Bogdanov教授らは，5-ヒドロキシトリプタミドをキレート化剤に導入したMRI造影剤，Gd-*bis*-5-HT-DTPAを合成している．合成されたGd-*bis*-5-HT-DTPAは，炎症部位に特異的に産生するミエロペルオキシダーゼの酸化作用によってオリゴマー化され（~5量体），緩和能がおおよそ2倍程度に増大する．さらに，そのオリゴマーが蛋白質に結合することによって高分子量化し，T_1緩和能がはじめにくらべておおよそ5.6倍に向上するMRI造影剤を合成した（**図2**）．このような酸化作用は，他のGd-DTPAを用いた場合には確認されず，5-ヒドロキシトリプタミドを有するGd-*bis*-5-HT-DTPAだけがミエロペルオキシダーゼの酸化力を受け，酸化カップリングを起こすことがわかっている[14]．

上記に示したMeade教授らのβ-ガラクトキシダーゼ感受性MRI造影剤は*in vitro*の試験結果であるが，後者のミエロペルオキシダーゼ感受性MRI造影剤は*in vivo*においてもその造影効果の増大が確認されている．

磁性微粒子を用いて，その緩和能を変化させる

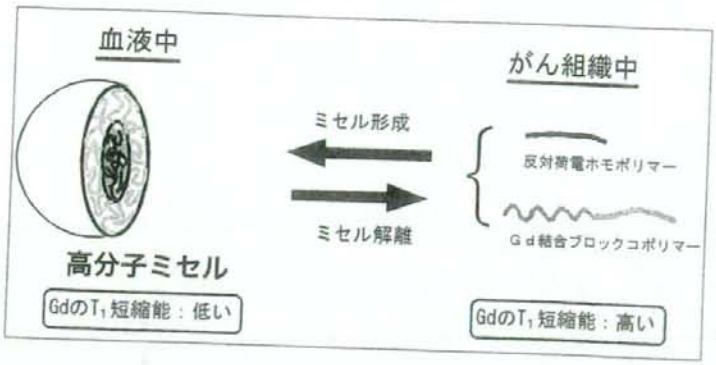

図4
ミセル構造形成・解離による
緩和能の制御

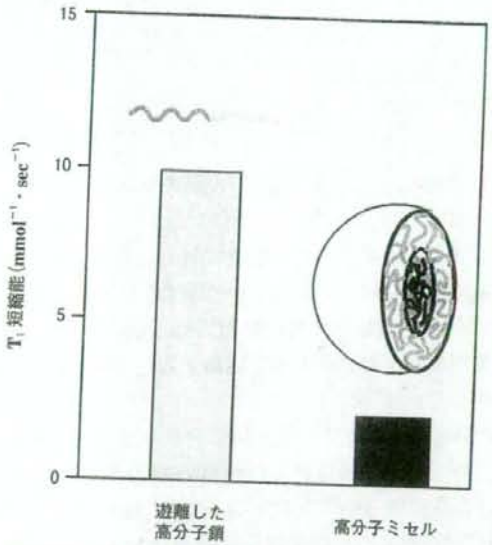

図5　高分子ミセルの形成・解離に基づく T_1 短縮能の変化

MRS(magnetic relaxation switching)法の研究が進められている．MRS法とは，磁性微粒子自身が有する T_2 緩和時間をターゲット部位で特定の反応によって T_2 緩和時間を早める，または遅くすることを目的とした方法である．具体的には，磁性微粒子をリバーシブルな反応を用いて自己凝集-解離を行う．先に述べたように，磁性微粒子はそのサイズによって磁気モーメントが変わる，つまり T_2 緩和時間が変化する．DNA-DNA 間，または蛋白質-蛋白質間の相互作用や，酵素を使うことでそれらの反応を起こすことが出来る．たとえば，アデノウイルスを用いると，100 nm ほどのサイズを有するアデノウイルス1分子が磁性微粒子の凝集を引き起こし，微粒子サイズがもとの 46 nm からおおよそ 10 倍の 500 nm 以上に変化する(**図3**)．これにより磁性微粒子の T_2 緩和時間は劇的に変化することが報告されている[15,16]．

以上にターゲット部位で造影効果を発揮する造影剤の例をキャリアの有無にかかわらずいくつかあげさせていただいた．今後，DDS ターゲティング技術のもと，キャリア設計とともにこうした造影剤の研究・開発が進められてゆくことであろう．

高分子ミセルを MRI 造影剤キャリアとした研究

最後に筆者らが行っている研究例を紹介させていただき，DDS と分子イメージングの接点を探ってゆきたい．

筆者らが設計した，高分子ミセルをキャリアとした MRI 造影剤は**図4**に示すような構造である．高分子ミセルはブロックコポリマー分子が多数会合してできる構造で，抗がん剤の場合はミセルの疎水性内核に抗がん剤を内封してターゲティングするとともに，疎水性場に薬物を保持することで薬物分子の体内での不活性化を抑制する効果もある[17,18]．MRI 造影剤においては，ミセル構造形成によってミセル内に位置する Gd キレートが周囲の水分子から隔離されることで，T_1 緩和時間短縮能(緩和能)が抑制されることを意図する．

すなわち，ミセル形態で血液を循環している間は，血液の画像コントラストは抑制される一方，がん組織内でミセル構造からブロックコポリマーに解離すると，Gd キレートは周囲の水に自由に接触す

ることができ，T_1緩和能を発揮してがん組織をコントラスト高く映し出す．がん組織内では分子量1万程度のブロックコポリマーでもEPR効果によって長時間組織内にとどまるのであるが，血液内でミセル構造が解離して生じたブロックコポリマーは，その分子量が腎臓の分画分子量より小さいので速やかに排出されて，血液の画像バックグラウンドは低く保たれる．すなわち，抗がん剤ターゲティングの場合には，ミセル内核に抗がん剤を封じ込めて高分子ミセルの特性による選択的送達のみであったが，MRI造影剤の場合にはこの選択的送達に加えて，ミセル構造の解離現象を画像選択性を得る手段として活用するのである．

この高分子ミセルシステムで，ポリアスパラギン酸にGdキレートを結合させてミセル内核高分子鎖とし，ポリアリルアミンを反対荷電ホモポリマーとしたものの結果を図5に示す．ミセル構造の形成する場合としない場合で約4倍のT_1短縮能の変化を得ることに成功した．この結果は，まだ*in vitro*のものであるが[19]，今後は，*in vivo*でのターゲティングとがん選択画像取得の最適化に進んでゆく．

文　献

1) Wang SC, Brasch RC et al. : Evaluation of Gd-DTPA-labeled dextran as an intravascular MR contrast agent : Imaging characteristics in normal rat tissues. Radiology 175 : 483-488, 1990.
2) Schmiedel U, Brasch RC et al. : Magnetic resonance imaging of myocardinal infarction using albumin-(Gd-DTPA), a macromolecular blood-volume contrast agent in a rat model. Investigative Radiology 22 : 713-721, 1987.
3) Unger E, Tilcock C et al. : Biodistribution and clearance of liposomal gadlinium-DTPA. Investigative Radiology 25 : 638-644, 1990.
4) Corot C, Meyer D et al. : Physical, chemical and biological evaluations of CMD-A2-Gd-DOTA. Acta Radiologica 38 : Supplement 412 : 91-99, 1997.
5) Modo M, Hoeehn M, Bulte JWM : Cellular imaging. Molecular Imaging 4 : 143-164, 2005.
6) Jaffer FA, Libby P, Weissleder R : Nanoparticle imaging of integrins on tumor cells. Circulation 116 : 1052-1061, 2007.
7) Lee JH, Huh YM, Jun YW, Seo JW, Jang JT et al. : Artificially engineered magnetic nanoparticles for ultra-sensitive molecular imaging. Nature Medicine 13 : 95-99, 2007.
8) Bogdanov Jr A, Wright SC, Marecos EM, Bogdanova A, Martin C et al. : A long-circulating co-polymer in "passive targeting" to solid tumors. J Drug Targeting 4 : 321-330, 1997.
9) Weissleder R, Mahmood U : Molecular imaging. Radiology 219 : 316-333, 2001.
10) Querol M, Bogdanov Jr A : Amplification strategies in MR imaging : activation and accumulation of sensing contrast agent. J Magn Reson Imaging 24 : 971-982, 2006.
11) Moats RA, Fraser SE, Meade TJ : A "smart" magnetic resonance imaging agent that reports on specific enzymatic activity. Angew Chem Int Engl 36 : 726-728, 1997.
12) Li WH, Fraser SE, Meade TJ : A calcium-sensitive magnetic resonance imaging contrast agent. J Am Chem Soc 121 : 1413-1414, 1999.
13) Major JL, Parigi G, Luchinat C, Meade TJ : The Syntheis and *in vitro* testing of a zinc-activated MRI contrast agent. PNAS 104 : 13881-13886, 2007.
14) Chen JW, Querol SM, Bogdanov Jr A, Weissleder R : Imaging of myeloperoxidase in mice by using novel amplifiable paramagnetic substrates. Radiology 240 : 473-481, 2006.
15) Perez JM, Josephson L, O'Loughlin T, Hogemann D, Weissleder R : Magnetic relaxation switches capable of sensing molecular interactions. Nature Biotechnology 20 : 816-820, 2002.
16) Perez JM, Simeone FJ, Saeki Y, Josephson L, Weissleder R : Viral-induced self-assembly of magnetic nanoparticles allows the detection of viral particles in biological media. J Am Chem Soc 125 : 10192-10193, 2003.
17) Yokoyama M et al. : Characterization and anti-cancer activity of micelle-forming polymeric anti-cancer drug, adriamycin-conjugated poly(ethylene glycol)-poly(aspartic acid) block copolymer. Cancer Res 50 : 1693-1700, 1990.
18) Opanasopit P et al. : Influence of serum and albumins from different species on stability of camptothecin-loaded micelles. J Controlled Release 104 : 313-321, 2005.
19) Nakamura E et al. : A polymeric micelle MRI contrast agent with changeable relaxivity. J Controlled Release 114 : 325-333, 2006.

Magnetic targeting after femoral artery administration and biocompatibility assessment of superparamagnetic iron oxide nanoparticles

Hui-Li Ma,[1] Xian-Rong Qi,[1] Wu-Xiao Ding,[1] Yoshie Maitani,[2] Tsuneji Nagai[2]
[1]*Department of Pharmaceutics, School of Pharmaceutical Sciences, Peking University, Beijing 100083, China*
[2]*Institute of Medicinal Chemistry, Hoshi University, Shinagawa-Ku, Tokyo 142-850, Japan*

Received 14 October 2006; revised 22 December 2006; accepted 30 January 2007
Published online 6 July 2007 in Wiley InterScience (www.interscience.wiley.com). DOI: 10.1002/jbm.a.31346

Abstract: Ferrofluids are attractive candidates for magnetic targeting system because of their fluidity and magnetism. The magnetic nanoparticles in ferrofluids should have combined properties of superparamagnetic behavior, target localization, and biocompatibility. The magnetic targeting and biocompatibility of superparamagnetic iron oxide nanoparticles stabilized by alginate (SPION-alginate) was investigated *in vitro* and *in vivo*. The localization of SPION-alginate by an external magnetic field *in vitro* was quantitatively evaluated by determining the iron content, and the results revealed that the localization ratio of SPION-alginate was 56%. Magnetic targeting of the SPION-alginate after femoral artery administration with the magnetic field in rats was quantitatively investigated by iron content and qualitatively confirmed by histological evaluation and magnetic resonance imaging. The ratio of iron content between the target site and the nontarget site were 8.88 at 0.5 h and 7.50 at 2 h, respectively. The viability of RAW264.7 cells and L929 cells was apparently unaltered upon exposure to SPION-alginate. The incubation with erythrocytes indicated that the SPION-alginate did not induce erythrocytes hemolysis and aggregation. In conclusions, the SPION-alginate had magnetic targeting with an external magnetic field and did not be detained at the injection site without the magnetic field. The SPION-alginate was generally considered to be biocompatible in cytotoxicity and hemolysis aspects. © 2007 Wiley Periodicals, Inc. J Biomed Mater Res 84A: 598–606, 2008

Key words: superparamagnetic iron oxide nanoparticles (SPION); magnetic targeting; biocompatibility; alginate; localization ratio

INTRODUCTION

Drug targeting always attracts the most interests from pharmaceutical researchers, among which magnetic drug targeting has been widely studied for the advantages to reduce the amount of drug needed and to reduce the adverse effect of drug. In magnetic targeting, a magnetic compound was injected into the systemic circulation, and then stopped with a powerful magnetic field in the target site.[1] Compared with other targeting vectors, such as ligand-targeting particulates and enzyme-triggered drug release system, magnetic targeting system is feasible to produce, reliable to control and can be specifically modified for drug delivery applications. Current applications of magnetic targeting system include magnetic delivery of chemotherapy drugs to tumors,[2–4] magnetic targeting of radioisotope,[1,5] magnetic hyperthermia,[6] magnetically enhanced gene therapy,[7] and magnetic embolization.[8] Some successes are achieved, but the results from both laboratory and clinical trials are far from satisfactory. Currently, one of the main problems is that the localization effect of magnetic carrier in target site with the magnetic field is not as good as expected.

Many factors, including physio-chemical properties of magnetic carrier, target sites, magnetic field, and the route of administration, can affect the magnetic targeting effect. When addressing the physiochemical properties of magnetic carrier, we have to consider the size, magnetization and matrix materials. Magnetic carriers can be grouped into ferrofluids, magnetic nanospheres, and magnetic microspheres according to the size from 10 nm to 100 μm. Ferrofluids are stable colloidal systems that com-

Correspondence to: X.R. Qi; e-mail: qixr2001@yahoo.com.cn
Contract grant sponsor: National High Technology Research and Development Program of China; contract grant number: 863 Program, No. 2003AA326020

posed of solid, magnetic, single-domain magnetic nanoparticles, typically between 3 and 15 nm in diameter, in a nonmagnetic solvent.[9] Because of the fluidity and magnetism of ferrofluids, they have been widely used in the magnetic targeting system. For biomedical applications, it is required that the magnetic nanoparticles should have combined properties of superparamagnetic behavior, high magnetic saturation, good stability, target localization ability, and biocompatibility. In our laboratory, a kind of ferrofluids, superparamagnetic iron oxide nanoparticles stabilized by alginate (SPION-alginate), was prepared successfully. They were composed of iron oxide (Fe_3O_4) with 5–10 nm core diameter and had good magnetic susceptibility.[10]

The magnetic field should be of sufficient strength to attract the magnetic particles into the desired area or target site. The higher magnetic flux density and magnetic gradient it is, the better the location effect is.[2] Because of the superparamagnetism and liquid state of ferrofluids, the magnetism of ferrofluids was usually weaker than that of magnetic microsphere. Therefore, a higher magnetic field is needed to attract or hold the injected ferrofluids to the target site.

The route of administration and target site can also greatly affect the magnetic targeting effect. If the target site is a part of reticuloendothelial system (RES), such as liver or spleen, most of magnetic carriers always accumulate in it by the passive targeting effect through intravenous injection. If the target site is a tumor outside RES, the passive accumulation in RES becomes a significant negative factor, and this is one reason why magnetic targeting carrier is still far from satisfactory. Compared with intravenous injection, the artery injection has more advantages, since the magnetic carriers have more chances to access to the target site, avoid clearance by RES, and then stopped by external magnetic filed.[3,4]

The term "biocompatibility" encompasses many different properties of the materials, however, two important aspects of the biomaterial screening refer to their *in vitro* cytotoxicity and blood compatibility behavior.[11] The cell lines of mouse fibroblasts (L929) and mouse macrophages (RAW264.7) were widely used in biocompatibility studies. L929 was recommended by many standard institutions as reference cell line for the cytotoxicity testing of polymers[12,13] and RAW264.7 was used for uptake iron oxide nanoparticles.[14]

In this study, we evaluated the magnetic targeting of SPION-alginate with the magnetic field both *in vitro* and *in vivo*. Biocompatibility of SPION-alginate was measured by hemolysis assay and erythrocytes aggregation assay, and *in vitro* cytotoxicity of L929 cells and RAW264.7 cells. Meanwhile, the labeling of RAW264.7 cells with SPION-alginate was examined.

MATERIALS AND METHODS

Chemicals and magnetic field

The SPION-alginate was a kind of superparamagnetic iron oxide nanoparticles stabilized by alginate macromolecules with good stability and good magnetism.[10] The SPION-alginate was prepared by a modified two-step coprecipitation method. The ferric and ferrous chlorides (molar ratio of 2:1.5) were dissolved in distilled water and chemical precipitation was achieved by adding 5 mol/L NaOH solution at 60°C. The sodium alginate solution was added to the suspension and was stirred vigorously for 30 min. The mixture was heated at 80°C with slow stirring for 1 h and then sonicated for 20 min. All the above processes were run under total N_2 protection. The obtained suspension was dialyzed against deionized water. Finally, the suspension was centrifuged at 10,000 rpm for 20 min to remove the solid material, and the black supernatant, namely SPION-alginate, was collected.

The SPION-alginate had a core (iron oxide nanoparticles) diameter of 5–10 nm, a hydrodynamic diameter of 193.8 nm, and ξ-potential of −67.5 mV. Saturation magnetization (Ms) of the SPION-alginate in suspension was 40 emu/g at 27°C. T1 relaxivity and T2 relaxivity in 0.9% NaCl solution determined by a 1.5 T MRI scanner at 20°C were 7.86 ± 0.20 s^{-1} mM^{-1} and 281.2 ± 26.4 s^{-1} mM^{-1}, respectively.[10]

A cuboid permanent neodymium iron boron magnet (NdFeB-permanent magnet) with length, width, and height of 33, 22, and 11 mm, respectively, was purchased from Beijing Sheng Magnetic Science & Tech (Beijing, China). The magnet with the surface magnetic field of 3500 G was used to produce the magnetic field. And all other reagents used were of analytical reagent grade.

Localization of SPION-alginate with magnetic field *in vitro*

The apparatus of localization of SPION-alginate with external magnetic field *in vitro* was shown in Figure 1. At first, the roller pump was turned on and the rate of distilled water (flow medium) was set to 8 mL/min and 0.5 mL SPION-alginate of 6.04 mg Fe/mL was injected at

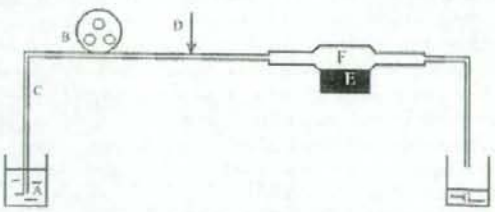

Figure 1. The *in vitro* apparatus of location of SPION-alginate with the external magnetic field. (A) flow medium (distilled water, 8 mL/min); (B) roller pump; (C) rubber tube; (D) injection site of SPION-alginate; (E) magnet; (F) glass tube; (G) eluted medium.

the injection part in the rubber tube. At 10 min after circulation, the glass tube with magnet was erected gently to pour the iron oxide particles unlocated tightly. The remnants of SPION-alginate in the glass tube captured by the magnet were separated, and 6*M* HCl solution was added to dissolve the iron oxide nanoparticles. The iron content was measured by *o*-phenanthroline method.[15] The ratio of iron content captured by the magnet to injected one was referred to as localization ratio *in vitro*. The experiment was repeated in triplicate.

Magnetic targeting evaluation *in vivo*

Male Sprague–Dawley rats weighing 250 ± 20 g were purchased from Department of Laboratory Animal Science of Peking University Health Science Center. NIH guidelines for the care and use of laboratory animals (NIH Publication #85-23 Rev. 1985) have been observed. Rats were divided into two groups randomly. One group was operated with magnetic field at the right thigh. Before the magnetic targeting of SPION-alginate was carried out, rats were anesthetized by intraperitoneal injection of 1.5 g/kg of ethyl carbamate. The right thigh was disinfected with iodine tincture and 70% alcohol by turns, 30,000 IU penicillin was given by intramuscular injection, and the femoral artery was separated. The SPION-alginate at a dose of 12 mg Fe/kg body weight was injected into the femoral artery at the right thigh under the magnetic field. When the magnetic targeting was performed, the distance between the magnet and the target site was 3 mm, the magnetic field intensity at the target site was 3000 G determined by Gaussmeter, and the magnetic field gradient was 2000 G/cm. The magnetization of SPION-alginate in suspension under the applied magnetic field of 3000 G was 36 emu/g.

After the magnetic targeting, rats were sacrificed by being cut abdominal aorta. The right thigh with magnetic field was referred to as the target site and the left thigh without magnetic field was referred to as the nontarget site in this paper. The right thigh (the target site), left thigh (the nontarget site), liver, and spleen of rats were immediately collected and frozen at −20°C until analysis. Concerning the thigh of rat, the leg was cut from inguinal groove to knee joint to get thigh part, and the thigh was decorticated, followed by removing the bone, separating the muscle of the thigh. Another group was operated without magnetic field at the right thigh, and other conditions were the same as the group with magnetic filed. The iron content in the right thigh, the left thigh, liver, and spleen were determined as follows. The tissues were digested in a beaker with the mixture acid of HNO_3-$HClO_4$ (4:1 v:v) for 48 h at room temperature, and then the solution was evaporated to dryness in sand bath at 100°C. Finally 37.5% HCl was added to the beaker to dissolve the solid and the iron content was determined by *o*-phenanthroline method. The ratio of iron content retained at the right thigh to that of injected was regarded as the localization ratio *in vivo*.

After the magnetic targeting, some of the right thigh (the target site) was intersected, embedded in 4% paraformaldehyde solution (pH 7.4), and then observed at light microscopy after Perls staining and hematoxylin and eosin (H&E) staining.

Ten hours after SPION-alginate application with or without magnetic field on the right thigh, magnetic resonance imaging (MRI) was performed on a 3.0 T clinical MR scanner (GE HD, Milwaukee, WI) with a GPFLEX coil. T2*-weighted gradient recalled echo (GRE) sequence with a coronary plane was used for imaging with the following parameters: repetition time (TR) of 460 ms; echo time (TE) of 6.6 ms; flip angle of 25°; bandwith of 62.5 kHz; field of view of 10 × 10 cm, slice thickness of 3 mm with no gap; matrix of 256 × 128.

Hemolysis assay *in vitro*

A hemolysis test was performed following the procedure reported previously.[16] The rabbit erythrocyte suspension in 0.9% NaCl (2% (v/v)) was prepared. The SPION-alginate of different concentrations, 0.9% NaCl solution (negative control group as 0% hemolysis) or distilled water (positive control group as 100% hemolysis) was added to the erythrocyte suspension and they were incubated for 3 h at 37°C. After centrifugation at 4000 rpm for 10 min, the absorbance of the supernatant was determined at 540 nm to evaluate the leakage of hemoglobin. Percentage of hemolysis was calculated by $(A_S - A_N - A_{SB})/(A_P - A_N) \times 100\%$, where A_S was the average absorbance of the SPION-alginate in erythrocyte suspension, A_N was the average absorbance of 0.9% NaCl solution in erythrocyte suspension (0% hemolysis), A_P was the average absorbance of distilled water in erythrocyte suspension (100% hemolysis). Because the SPION-alginate still had some extent absorbance at 540 nm after centrifugation, so the average absorbance of SPION-alginate only in 0.9% NaCl solution (A_{SB}) is introduced to the equation in order to eliminate the effect of SPION-alginate itself. The experiment was done in triplicate.

Erythrocytes aggregation assay

Rabbit erythrocytes suspension 200 μL was mixed with the indicated amount of SPION-alginate and incubated for 1 h at 37°C in a 24-well plate. The plate was examined by an inverted microscope (Leica DMIRE2, Germany).

Cell culture

L929 cells and RAW264.7 cells were cultured in RPMI 1640 medium (Gibco-Invitrogen, NY) supplemented with 10% (v/v) heat-inactivated newborn calf serum (NCS) (Hyclone, USA), 200 U/mL penicillin, 100 U/mL streptomycin, and 0.11 mg/mL sodium pyruvate. Cells were all maintained in a 5% CO_2 atmosphere at 37°C.

In vitro cytotoxicity evaluation

To determine cytotoxicity, a 3-(4,5-dimethylthiazol-2-yl)-2,5-diphenyl tetrazolium bromide (MTT) assay was performed.[17] The cells were plated at a density of 5×10^4 cells/well for RAW264.7 and 3×10^4 cells/well for L929 in 96-well plate and cultured for 24 h at 37°C in a 5% CO_2 atmosphere. For cytotoxicity without NCS, the medium in

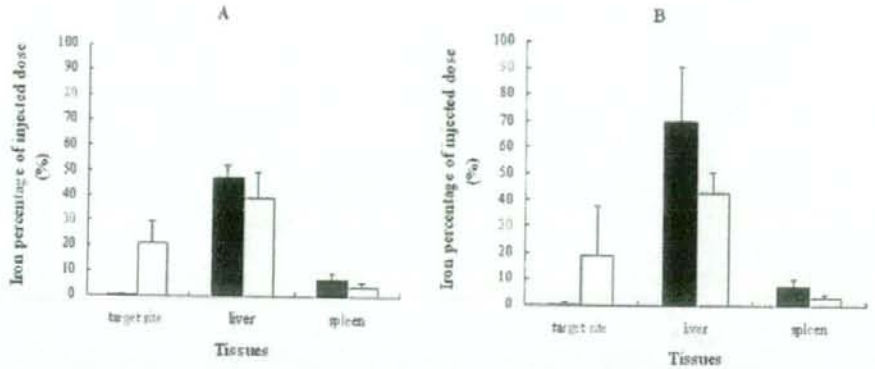

Figure 2. The iron percentage of injected SPION-alginate in target site, liver, and spleen with (□) or without (■) 3500 G magnetic field at 0.5 h (A) or 2 h (B) after femoral arterial injection of SPION-alginate at a dose of 12 mg Fe/kg. Data represent mean ± SD ($n = 3$).

the wells was replaced with 90 μL RPMI 1640 medium, 24 h later, 10 μL serial dilutions of the SPION-alginate were added to cells for 24 h with final iron concentrations from 6.25 to 100.0 μg/mL, and 10 μL RPMI 1640 medium was added to cells as control sample. For cytotoxicity with NCS, the medium in the wells was replaced with 90 μL RPMI 1640 medium with 10% NCS and 10 μL serial dilutions of SPION-alginate were added with the same iron concentrations as mentioned earlier for 24 h. The cells were washed once with phosphate-buffered saline (PBS, pH 7.4) and replenished with 100 μL medium, and then 10 μL MTT solution (Sigma, USA) at 5 mg/mL in saline solution was added to each well. After 4 h of incubation, the medium was removed and formazan crystals were solubilized with dimethylsulphoxide (DMSO) for 10 min at room temperature. The absorbance of each well was then measured on a microplate reader (Bio-Rad Model 550, USA) at a wavelength of 570 nm, with 655 nm as a reference wavelength. The relative cell viability (%) related to control wells was calculated by $(A_{test}/A_{control}) \times 100\%$, where A_{test} was the absorbance of the test sample and $A_{control}$ was the absorbance of control sample. The experiments were run in hexakis and were repeated three times.

Cell labeling with SPION-alginate

RAW264.7 cells were seeded at a density of 5×10^4 cells/mL in 35-mm culture plate at 37°C in a 5% CO_2 atmosphere. After 24 h, the SPION-alginate was added to cells with final iron cation concentrations ranging from 12.5 to 50.0 μg/mL for various incubation times (1–24 h). And then the cells were washed with PBS to remove excess SPION-alginate. For Prussian blue staining, which indicated the presence of iron, the cells were fixed with 4% glutaraldehyde (Merck, Germany) for 10 min and were washed with PBS, followed by incubation with 2% potassium ferrocyanide in 6% HCl for 30 min. After the wash, they were counterstained with nuclear fast red for 5 min.[18] The specimens were then examined under a light microscope (Olympus BH2, Japan).

RESULTS

Localization of SPION-alginate with magnetic field *in vitro*

From the iron content of SPION-alginate captured by the magnet, the localization ratio *in vitro* was (56 ± 5.1)% ($n = 3$).

Magnetic targeting evaluations *in vivo*

Figure 2 showed the iron accumulation in target site, liver and spleen with or without magnetic field via femoral artery injection of SPION-alginate at a dose of 12 mg Fe/kg. At 0.5 h [Fig. 2(A)] and 2 h [Fig. 2(B)] after injection, the localization ratios *in vivo* were about 20%, the iron contents in the right thigh (the target site) with magnetic field were significantly higher than those in the left thigh without magnetic field, and at the same time, the iron contents in liver and spleen with magnetic field were lower than those without magnetic field. The results suggested that the SPION-alginate had some magnetic targeting effect *in vivo*.

In Figure 3, the ratios of iron content (right thigh/left thigh) at 0.5 and 2 h after injection were 1.17 and 1.33 without magnetic field, indicated the SPION-alginate did not be detained in injection site. On the contrary, the ratios of iron content at 0.5 and 2 h after injection were 8.88 and 7.50 with magnetic field, showed the SPION-alginate could be retained at target site with the magnetic field.

With magnetic field at 0.5 h, the femoral artery was filled with iron oxide while the femoral vein was not [Fig. 4(A)], providing a visual evidence for the magnet localization ability of SPION-alginate. Without magnetic field at 0.5 h, the iron oxide was not found

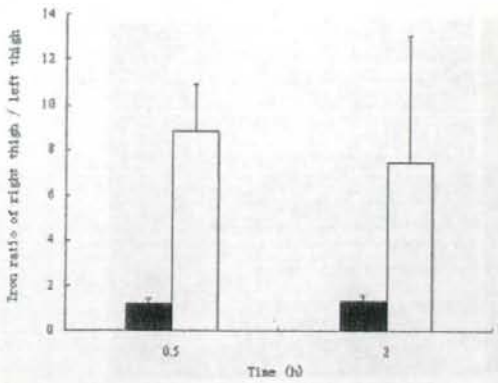

Figure 3. Iron ratio of right thigh (target site) and left thigh (nontarget site) with (□) or without (■) magnetic field at 0.5 and 2 h after injection of SPION-alginate. Data represent mean ± SD ($n = 3$).

both in femoral artery and in femoral vein [Fig. 4(B)], suggesting that no SPION-alginate was detained in the vascular system without magnetic field.

Iron oxide is well-known to significantly shorten the transverse relaxation times (T2 or T2*) with a subsequent loss of MR signal intensity.[19] Therefore, iron oxide can result in a strong decrease in signal intensity (negative enhancement) of the tissues where they accumulate. Figure 5(A) on T2*-weighted image showed the localization of the iron oxide nanoparticles at the right thigh (circle) with the magnetic field, but no localization was showed without magnetic field [Fig. 5(B)].

Hemolysis and erythrocytes aggregation analysis

The leakage of hemoglobin was used to quantify the erythrocytes damage by the SPION-alginate. As shown in Table I, the hemolysis of three preparations of SPION-alginate with different series concentrations were below 5%. So the SPION-alginate did not show hemolytic effect, that is no destruction to the red blood cell membranes. Furthermore, erythrocytes were incubated with the SPION-alginate for 1 h at 37°C, and no aggregation was observed.

Cytotoxicity analysis

The results of the MTT assay indicated that the viability of L929 and RAW264.7 apparently unaltered

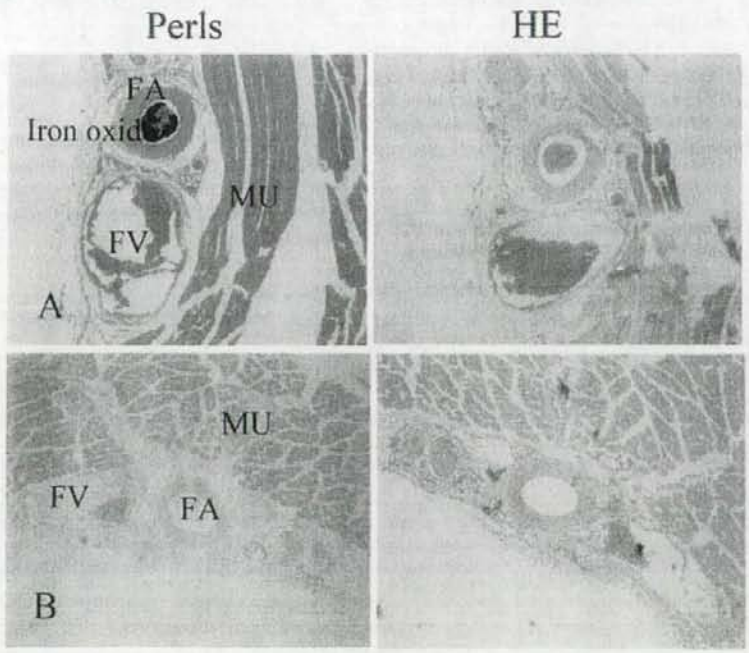

Figure 4. Micrographs of rat right thigh (target site) after femoral arterial injection with magnetic field (A) or without magnetic field (B) at 0.5 h. The tissues were stained with H&E and Perls. FA, femoral artery; FV, femoral vein; MU, muscle (×40 magnification). [Color figure can be viewed in the online issue, which is available at www.interscience.wiley.com.]

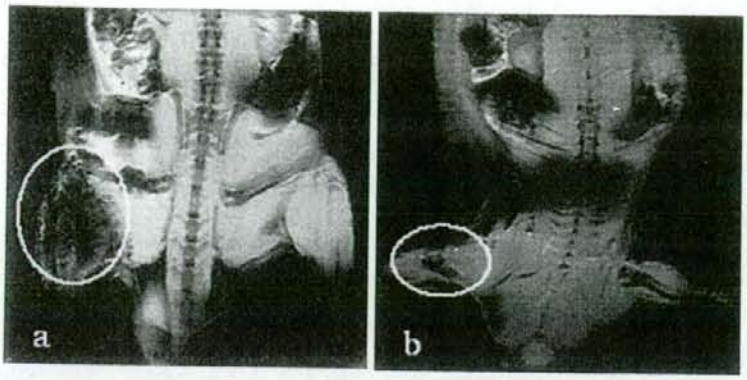

Figure 5. T2*-weighted MRI of right thigh after femoral injection of SPION-alginate with 0.5 h exposure time to magnetic field (A) or not (B). The images were taken at 10 h after injection, which still showed accumulation of iron oxide in target site with the magnetic field, since the strong signal intensity decreased (white circle in A). But the iron oxide did not accumulate in target site (white circle in B), which could be attributed to the slight change of signal intensity without the magnetic field.

upon exposure to various concentrations of SPION-alginate for 24 h with or without NCS (Fig. 6).

Cell labeling with SPION-alginate

Following 1–24 h incubation with SPION-alginate, almost all RAW264.7 cell labeling were achieved. It was evident that the labeled RAW264.7 cells contained abundant Fe_3O_4 nanoparticles in the cytoplasm after incubation with the iron concentration of 12.5, 25.0, and 50.0 μg/mL. The SPION-alginate was internalized into RAW264.7 cells in a concentration- and time- dependent manner (Fig. 7). At a concentration of 25.0 μg/mL, cells started to internalize iron particles already after 1 h incubation [Fig. 7(B)] and the internalization was increased from 1 to 24 h incubation [Fig. 7(C–E)]. For 5 h of incubation at different concentrations, it showed the amount of Prussian blue positive particles in cytoplasma as follow: 50.0 > 25.0 > 12.5 μg/mL. However, no stainable iron was detected in the control cells [Fig. 7(A)].

TABLE I
Hemolysis Percentage of Rabbit Erythrocytes at 37°C After 3 h Incubation With Different Concentrations of SPION-Alginate

SPION-Alginate Concentration (mg Fe/mL)		
Bulk Suspension	Final Suspension	Hemolysis (%)
2.08	0.04	−0.34 ± 0.16
2.08	0.08	0.71 ± 0.78
2.08	0.12	0.29 ± 0.16
2.08	0.17	1.15 ± 0.34
2.08	0.21	2.08 ± 1.48
3.62	0.07	0.23 ± 1.15
3.62	0.14	0.62 ± 1.41
3.62	0.22	1.03 ± 0.70
3.62	0.29	3.19 ± 1.56
3.62	0.36	3.19 ± 1.09
5.74	0.11	1.38 ± 0.96
5.74	0.23	0.62 ± 0.53
5.74	0.34	2.21 ± 0.89
5.74	0.46	2.35 ± 1.74
5.74	0.57	3.24 ± 0.26

Data represent mean ± SD (n = 3). The hemolysis >5% was regarded as erythrocytes hemolysis.

DISCUSSION

To optimize magnetic targeting, several factors need to be considered, (a) the magnetic field, including magnetic intensity and magnetic intensity gradient, should be of sufficient strength to attract the magnetic nanoparticles into the target site; (b) the

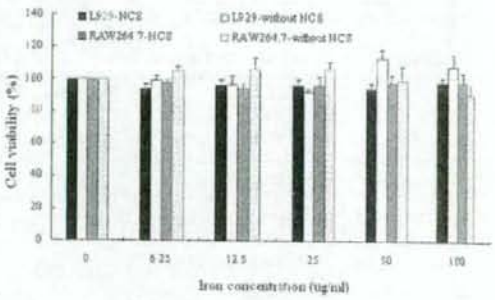

Figure 6. Viability of L929 cells and RAW264.7 cells exposed to SPION-alginate for 24 h at various iron concentrations ranging from 6.125 to 100.0 μg/mL. Cell viability is expressed as the mean ± SD of the percentage of absorbance of controls, where 100% equals viability of the control cells. The experiments were performed in hexakis and were repeated three times.

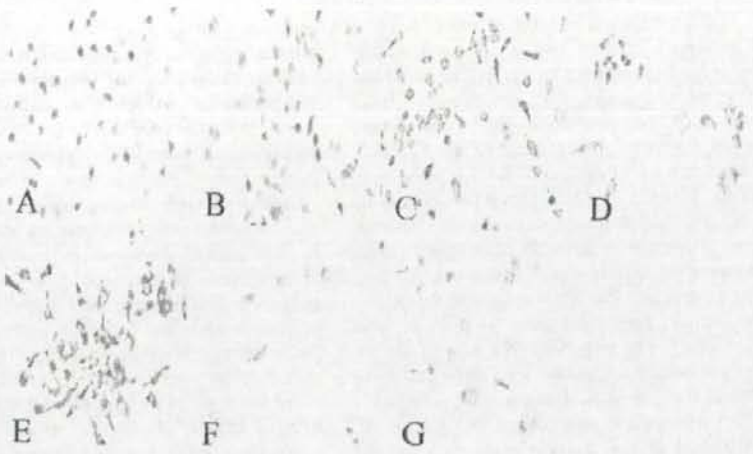

Figure 7. Photomicrographs of Prussian blue stained labeled and control RAW264.7 cells. Cells were cultured with different concentrations of SPION-alginate and harvested after different incubation times. Note the abundant iron particles in the cytoplasm of the cells (blue dots). (A) control; (B) SPION-alginate 25.0 μg/mL, 1 h; (C) SPION-alginate 25.0 μg/mL, 5 h; (D) SPION-alginate 25.0 μg/mL, 12 h; (E) SPION-alginte 25.0 μg/mL, 24 h; (F) SPION-alginate 12.5 μg/mL, 5 h; (G) SPION-alginate 50.0 μg/mL, 5 h (×400 magnification). [Color figure can be viewed in the online issue, which is available at www.interscience.wiley.com.]

magnetic particles should be of a suitable size with good magnetization and biocompatibility; (c) the method of injection should have good access to the target site and the particles should avoid clearance by RES.

In the magnetic targeting study, we employed three methods: iron content measurement, histological evaluation, and MRI. The SPION-alginate could be retained in the target site under the magnetic field with the localization ratio of 56% *in vitro* and the localization ratio of 20% *in vivo*, while reducing accumulation in the liver and spleen (Fig. 2). In addition, without magnetic field, the SPION-alginate would not be retained at the injection site (Fig. 4). The localization ratio of SPION-alginate *in vivo* was lower than that *in vitro* under the same magnetic field. One of the most important factors affecting the localization ratio of SPION-alginate *in vivo* was the rapid blood flow rate approximately 30 cm/s in large arteries.[20] Hence, part of the SPION-alginate would be flushed by the high blood flow rate which caused the decrease of the localization ratio *in vivo*. In addition, the SPION-alginate was still be phagocytosed by RES although by the artery administration.

Without magnetic field, the accumulation of SPION-alginate in liver (47.54%) and in spleen (6.66%) by femoral artery administration at 0.5 h was significantly lower than that in liver (>80%) and in spleen (10%) by vein administration at 0.5 h (data were not shown), which proved that artery injection was more advantageous than vein injection when the SPION-alginate was targeted to the sites other than liver and spleen. Furthermore, it was reported that intravenous infusion of magnetic drug particles was ineffective to make tumor remission, but the combination of artery infusion with a magnetic field was safe and effective.[2] At present, intraarterial injection of chemotherapeutic agents is approved and well accepted for treatment of liver metastases, and it has occasionally been used for other tumor types such as inoperable head and neck tumors.[21] Many other studies also confirmed the efficacy of arterial administration of magnetic targeting.[3,4,22,23] Currently, the doxorubicin hydrochloride absorbed to magnetic targeted carriers (MTC-DOX) is under clinical investigation for the treatment of patients with primary hepatocellular carcinoma (HCC). It was reported that the particles could be retained at HCC under the applied magnetic field after 28 days by intraarterial administration in human clinical trials.[21] Furthermore, a multicenter, phase I/II trial of hepatic intraarterial deliver of MTC-DOX in patients with HCC and a phase I/II dose escalation study of MTC-DOX in patients with metastatic liver tumors have been undertaken, the results indicated that MTC-DOX could be localized regionally following intraarterial administration without clinically significant toxicities in all cases.[4,23]

The magnetization of the particles was related to the magnetic field strength and the magnetic field gradient. The higher magnetic flux density and magnetic gradient it is, the better the location effect is.[2] Until now, the maximum magnetic field reported was a magnetic flux density of a maximum of 1.7

and 1.0 T at 10 mm below the tip of the pole shoe produced by electric magnet[2] and a remanence field of 1.3 T by NdFeB-permanent magnet.[24] In previous studies, it was suggested that a magnetic field strength of 0.8 T was sufficient to exceed linear blood flow in the intratumoral vasculature.[20] However, a magnetic field of only 250–1000 G has been used to locate the iron oxide particles (0.5–5 μm) in liver and lung.[25] One of the most important reasons for the great difference in strength of magnetic field used above was the difference of the magnetization of iron oxide particles. The high magnetic flux density focused onto the target area is one of the obstacles for effectively targeting. The use of larger particles, as previously suggested by Lübbe and Bergemann,[26] and the use of a stronger magnetic field, are the two approaches to overcome this problem. If the magnetization of the particle is low, a higher magnetic field is needed and vice versa. Therefore, the selection of magnetic field depends on the magnetization of the magnetic carrier. NdFeB-permanent magnet with the surface magnetic field of 3500 G and with the magnetic gradient of 2000 G/cm was used in this study. We achieved a high concentration of iron oxide within the target site after femoral artery administration of the SPION-alginate, which was seen by quantitative evaluation of iron (Figs. 2 and 3), histological (Fig. 4) and MRI (Fig. 5) methods.

As respect to the time of magnetic field added, the shortest time reported was 15 min and the longest time was 24 h.[22,24] In this study, the SPION-alginate had some magnetic targeting effect under the magnetic field at 0.5 h and as the time was prolonged to 2 h, it did not produce better magnetic target. It might be explained that the iron oxide of strong magnetism would soon be absorbed under the magnetic field of 3500 G, while those of poor magnetism would not be absorbed as the time increased and could still be phagocytosed by RES. We speculate that the time of magnetic field added depends both on the magnetization of the particles and the intensity of magnetic field. The higher magnetization of particles and the higher intensity of magnetic field, the shorter time of magnetic field.

Concerning magnetic targeting, there are many practical applications of the magnetic nanoparticles, such as magnetic drug targeting,[2–5,20,23,24] magnetic fluid hyperthermia,[6] and MRI.[9,19] The magnetic nanoparticles can act as carriers of drug and gene for site-specific drug and gene delivery. For example, the SPION-alginate can be functionalized with specific drug like chemotherapeutic drugs for chemical therapy or radioactive isotope for radionuclide therapy. Another promising application of the magnetic nanoparticles is magnetic fluid hyperthermia as one of cancer therapy strategies. When the magnetic carrier is localized at the target site with the applied magnetic field, some heat is generated under an alternating magnetic field due to magnetic hysteresis of magnetic particles. Furthermore, the magnetic nanoparticles can result in a strong decrease in MR signal intensity (negative enhancement) of the tissues where they accumulate. Therefore, it will play an important role in MR contrast imaging to better discriminate healthy and pathological tissues.

Although some encouraging data were achieved in this study, there are many issues to be further investigated on magnetic targeting. For example, a potential complication that could arise with the use of ferrofluid is the fact that an embolization process could occur after magnetic targeting, and the embolization is to some extent favorable for cancer treatment because of their cut-off of the blood and nutrition of tumor.[8] However, it was reported that the therapeutic effect resulted from the action of the chemotherapeutic agent itself, rather than intratumoral embolization by the particles.[2] On the other hand, the localization accuracy of the particles at the target site needs to be optimized, and the design of the magnetic field with greater magnetic field intensity and magnetic field gradient is quite important and needs to be improved.

Compared with the corresponding control cells, no significant change was observed in the viability of RAW264.7 cells and L929 cells with various different concentrations of SPION-alginate for 24 h incubation with or without serum (Fig. 6). Hence, we considered that the SPION-alginate was not toxic to RAW264.7 cells and L929 cells. In addition, the SPION-alginate did not induce erythrocytes hemolysis and erythrocytes aggregation. Accordingly, the SPION-alginate was generally considered to be of good biocompatibility.

Figure 7 showed that the labeled RAW264.7 cells contained abundant Fe_3O_4 nanoparticles in the cytoplasm after 1–24 h incubation with the various concentrations of SPION-alginate. The high RAW264.7 labeling efficiency with the SPION-alginate seems to be related firstly to the nonspecific process of nanoparticles adsorption on the cell membrane in the form of clusters, secondly to their subsequent internalization into endosomes, as introduced by other authors.[14,27] The interaction of the SPION-alginate with living cells should be further investigated. Moreover, the Fe_3O_4 nanoparticles bound to alginate macromolecule strands like "fruit" in the "tree," not simply coated by the polymer. They were visually confirmed by atomic force microscopy.[10] It is indicated that alginate would not hamper their interactions with cell membrane, which could be caused by steric coating effect. Besides, the good bioadhesion property of alginate is beneficial to the adsorption of SPION-alginate on the cell membrane. Because of the nonspecific cellular uptake mediated by adsorptive

endocytosis, the SPION-alginate labeling may be nonspecific and potentially applicable to a wide variety of cells, making it useful for cellular imaging strategies.

CONCLUSIONS

With magnetic field, the SPION-alginate had a localization ratio of 56% *in vitro* and 20% *in vivo*, meanwhile, the contents of the SPION-alginate in liver and spleen were reduced. The magnetic targeting effect was established by evaluating the iron content ratio of target site/nontarget site, and was visually confirmed by histological evaluation and MRI. Furthermore, the SPION-alginate was considered to be biocompatible in respects of cytotoxicity and hemolysis.

References

1. Häfeli UO. Magnetically modulated therapeutic systems. Int J Pharm 2004;277:19–24.
2. Alexiou C, Arnold W, Klein RJ, Parak FG, Hulin P, Bergemann C, Erhardt W, Wagenpfeil S, Lübbe AS. Locoregional cancer treatment with magnetic drug targeting. Cancer Res 2000;60:6641–6648.
3. Leakakos T, Ji C, Lawson G, Peterson C, Goodwin S. Intravesical administration of doxorubicin to swine bladder using magnetically targeted carriers. Cancer Chemother Pharmacol 2003;51:445–450.
4. Just R, Hoh C, Vogl T, Neese P, Doemeny J, Schechter M, Varney R, Stanton W, Schiemann M, Goldfarb P. A phase I/II single arm trial to determine the safety, tolerability, and biological activity of intrahepatic delivery of doxorubicin hydrochloride adsorbed to magnetic targeted carriers (MTX-DOX) in patients with metastatic tumors in the liver. Eur J Cancer Suppl 2003;1:S292–S293.
5. Häfeli U, Pauer G, Failing S, Tapolsky G. Radiolabeling of magnetic particles with rhenium-188 for cancer therapy. J Magn Magn Mater 2001;225:73–78.
6. Jordan A, Scholz R, Maier-Hauff K, Johannsen M, Wust P, Nadobny J, Schirra H, Schmidt H, Deger S, Loening S, Lanksch W, Felix R. Presentation of a new magnetic field therapy system for the treatment of human solid tumors with magnetic fluid hyperthermia. J Magn Magn Mater 2001;225:118–126.
7. Scherer F, Anton M, Schillinger U, Henke J, Bergemann C, Krüger A, Gänsbacher B, Plank C. Magnetofection: Enhancing and targeting gene delivery by magnetic force in vitro and in vivo. Gene Ther 2002;9:102–109.
8. Widder KJ, Senyei AE, Scarpelli GD. Magnetic microspheres: A model system for site specific drug delivery in vivo. Proc Soc Exp Biol Med 1978;158:141–146.
9. Wang YX, Hussain SM, Krestin GP. Superparamagnetic iron oxide contrast agents: Physicochemical characteristics and applications in MR imaging. Eur Radiol 2001;11:2319–2331.
10. Ma HL, Qi XR, Maitani Y, Nagai T. Preparation and characterization of superparamagnetic iron oxide nanoparticles stabilized by alginate. Int J Pharm 2007;333:177–186.
11. Sgouras D, Duncan R. Methods for the evaluation of biocompatibility of soluble synthetic polymers which have potential for biomedical use: 1-Use of the tetrazolium-based colorimetric assay (MTT) as a preliminary screen for evaluation of in vitro cytotoxicity. J Mater Sci: Mater Med 1990;1:61–68.
12. Biological Evaluation for Medical Devices, Part 5: Tests for Cytotoxicity: In Vitro Methods. United States Pharmacopeia XXIII, 1995.
13. Biological Evaluation of Medical Devices. Part 5: Test for In Vitro Cytotoxicity. ISO 10993-5 (EN 30993-5), 1999.
14. Wilhelm C, Billotey C, Roger J, Pons JN, Bacri JC, Gazeau F. Intracellular uptake of anionic superparamagnetic nanoparticles as a function of their surface coating. Biomaterials 2003;24:1001–1011.
15. Hagar W, Vichinsky EP, Theil EC. Liver ferritin subunit ratios in neonatal hemochromatosis. Pediatr Hematol Oncol 2003;20:229–235.
16. Regulations of new drug license application in China.State Food and Drug Administration in China; 1999. p 24.
17. Mosmann T. Rapid colorimetric assay for cellular growth and survival: Application to proliferation and cytotoxicity assays. J Immunol Methods 1983;65:55–63.
18. Arbab AS, Bashaw LA, Miller BR, Jordan EK, Lewis BK, Kalish H, Frank JA. Characterization of biophysical and metabolic properties of cells labeled with superparamagnetic iron oxide nanoparticles and transfection agent for cellular MR imaging. Radiology 2003;229:838–846.
19. Saini S, Stark DD, Hahn PF, Wittenberg J, Brady TJ, Ferrucci JT. Ferrite particles: A superparamagnetic MR contrast agent for the reticuloendothelial system. Radiology 1987;162:211–216.
20. Senyei A, Widder K, Czerlinski C. Magnetic guidance of drug carrying microspheres. J Appl Phys 1978;49:3578–3583.
21. Link KH, Kornmann M, Formenti A, Leder G, Sunelaitis E, Schatz M, Pressmar J, Beger HG. Regional chemotherapy of non-resectable liver metastases from colorectal cancer-literature and institutional review. Langenbecks Arch Surg 1999;384:344–353.
22. Rudge S, Peterson C, Vessely C, Koda J, Stevens S, Catterall L. Adsorption and desorption of chemotherapeutic drugs from a magnetically targeted carrier (MTC). J Control Release 2001;74:335–340.
23. Koda J, Venook A, Walser E, Goodwin S. A multicenter, phase I/II trial of hepatic intra-arterial delivery of doxorubicin hydrochloride adsorbed to magnetic targeted carriers in patients with hepatocellular carcinoma. Eur J Cancer 2002;38(Suppl 7):S18.
24. Schulze K, Koch A, Schöpf B, Petri A, Steitz B, Chastellain M, Hofmann M, Hofmann H, von Rechenberg B. Intraarticular application of superparamagnetic nanoparticles and their uptake by synovial membrane—An experimental study in sheep. J Magn Mag Mater 2005;293:419–432.
25. Goodwin S, Peterson C, Hoh C, Bittner C. Targeting and retention of magnetic targeted carriers (MTCs) enhancing intra-arterial chemotherapy. J Magn Mag Mater 1999;194:132–139.
26. Lübbe AS, Bergemann C.Selected preclinical and first clinical experiences with magnetically targeted 4'-epidoxorubicin in patients with advanced solid tumors. In: Häfeli U, Schütt W, Teller J, Zborowski M, editors. Scientific and Clinical Application of Magnetic Carriers. New York:Plenum; 1997. p 457–480.
27. Wilhelm C, Gazeau F, Roger J, Pons JN, Bacri JC. Interaction of anionic superparamagnetic nanoparticles with cells: Kinetic analyses of membrane adsorption and subsequent internalization. Langmuir 2002;18:8148–8155.

Available online at www.sciencedirect.com
ScienceDirect
International Journal of Pharmaceutics 354 (2008) 217–226
INTERNATIONAL JOURNAL OF PHARMACEUTICS
www.elsevier.com/locate/ijpharm

Pharmaceutical Nanotechnology

Superparamagnetic iron oxide nanoparticles stabilized by alginate: Pharmacokinetics, tissue distribution, and applications in detecting liver cancers

Hui Li Ma [a], Yu Feng Xu [b], Xian Rong Qi [a,*], Yoshie Maitani [c], Tsuneji Nagai [d]

[a] *Department of Pharmaceutics, School of Pharmaceutical Sciences, Peking University, Beijing 100083, China*
[b] *Department of Radiology, First Hospital, Peking University, Beijing 100034, China*
[c] *Institute of Medicinal Chemistry, Hoshi University, Shinagawa-Ku, Tokyo 142-8501, Japan*
[d] *The Nagai Foundation Tokyo, Hon-Komagome, Bunkyo-ku, Tokyo 113-0021, Japan*

Received 13 August 2007; received in revised form 18 November 2007; accepted 20 November 2007
Available online 28 November 2007

Abstract

The objectives of this study were to describe the pharmacokinetics and tissue distribution of superparamagnetic iron oxide nanoparticle (SPIO) stabilized with alginate (SPIO-alginate), and investigate its potential in detecting liver cancers as a newly developed magnetic resonance (MR) contrast agent. Pharmacokinetics and tissue distribution of SPIO-alginate were investigated in Sprague–Dawley rats. The results showed that SPIO-alginate was eliminated rapidly from serum with the half-life of 0.27 h at 109.5 μmol Fe/kg and accumulated dominantly in liver and spleen with a total percentage of more than 90% of dose after intravenous injection. The studies of pharmacokinetics and distribution of SPIO-alginate in rats indicated the MR contrast agent, based on SPIO, mainly accumulating in targeting organs that contain phagocytosing cells, i.e. liver and spleen. The efficacies in detecting hepatocellular carcinoma (HCC) of rat with primary liver cancer and xenograft liver cancers of rabbit were investigated before and after injection of SPIO-alginate. The signal intensity of liver parenchyma in rabbit with VX2 tumor after injection of SPIO-alginate was reduced sharply resulting in a significant contrast between liver parenchyma and tumor. Detection of the HCC in rat model was also demonstrated. The present study provides evidence that SPIO-alginate might have the ability to improve the detection of liver tumors as an MR contrast agent, and the efficacy is associated with the SPIO specifically located in Kupffer cells in hepatic sinusoid.

Keywords: Superparamagnetic iron oxide nanoparticles (SPIO); Pharmacokinetics; Distribution; Liver cancers; Contrast agent; Alginate

1. Introduction

MR imaging is one of the most useful non-invasive methods in the field of diagnostic imaging, which is characterized by its high resolution of soft-tissues and by its non-exposure to radiation. To better differentiate healthy and pathological tissues, paramagnetic gadolinium based contrast agents which shorten the longitudinal relaxation time (T1) and increase the contrast of the image (positive enhancement) are mainly used today (Weinmann et al., 2003). Compared to gadolinium based contrast agents, SPIO can produce enhanced relaxation rates in specific organs at lower dose than paramagnetic ions, because of their larger magnetic moment (Corot et al., 2006; Wang et al., 2001). Generally speaking, the transverse relaxation (T2 and T2*) effect of SPIO is mostly utilized in detection of liver lesions by MR imaging. SPIO are distributed in reticuloendothelial cells, such as Kupffer cells (KCs), according to phagocytic activity, and cause local field inhomogeneities that produce rapid dephasing of neighboring proton spins, resulting in a shortening of T2 relaxation times. In contrast, liver tumors such as metastatic liver cancer and HCC cannot absorb these agents because of the lack of reticuloendothelial cells. Therefore, the contrast between tumor tissue and surrounding normal liver tissue is enhanced because of signal loss in the liver tissue (Saini et al., 1987). Hence, SPIO can produce a strong decrease in MR signal intensity (negative enhancement) in the tissues where they accumulate, such as the liver, spleen, bone marrow, and lymph node (Saini et al., 1987; Corot et al., 2006).

* Corresponding author. Tel.: +86 10 82801584; fax: +86 10 82802791.
E-mail address: qixr2001@yahoo.com.cn (X.R. Qi).

0378-5173/$ – see front matter © 2007 Elsevier B.V. All rights reserved.
doi:10.1016/j.ijpharm.2007.11.036

Until now, two SPIO preparations have already been approved for clinical use, especially for liver MR imaging, such as Ferumoxides (i.e. Endorem® in Europe, Feridex® in the USA and Japan, Advanced Magnetics, USA) coated with dextran (Weissleder et al., 1989), and Ferucarbutran (i.e. Resovist® in Europe and Japan, Schering, Germany) coated with carboxydextran (Reimer et al., 1995). Furthermore, several SPIO preparations have been investigated in human for imaging applications, such as VSOP-C184, a very small SPIO coated with citrate (Taupitz et al., 2004), and Feruglose (Clariscan; Amersham Health, Oslo, Norway) where iron oxide particles have been stabilized with oxidized starch that consist of carbohydrate-polyethylene glycol (Kellar et al., 2000).

In our previous work, SPIO stabilized with alginate (SPIO-alginate) have been successfully prepared (Ma et al., 2007) and the SPIO-alginate have good biocompatibility and some magnetic targeting under the magnetic field (Ma et al., 2007a). As the coating material of iron oxide, alginate is known for binding many multivalent ions *in vitro* such as Ca^{2+}, Ba^{2+}, Fe^{2+}, and Fe^{3+}. The high stability of SPIO-alginate is probably caused by the binding of the carboxyl group of alginate to iron oxide nuclei (Ma et al., 2007). It was reported that the absorption of Fe, Cr, and Co was significantly reduced after oral administration of sodium alginate in rats, while Ca and Zn absorption was not affected (Harmut-Hoene and Schelenz, 1980). Hence, it is necessary to investigate the effect of alginate and SPIO-alginate on the iron level *in vivo*, even if some COO^- terminals of alginate have been bound to iron oxide in SPIO-alginate.

We presumed that using SPIO-alginate as an intravenous contrast medium, detection of malignant liver lesions by MR imaging might be improved. Once iron oxide particles are taken up by the macrophages situated in the liver of reticuloendothelial system (RES) but not by tumor cells, the contrast between liver parenchyma and liver lesion would significantly increase, which is caused by the distinct signal loss in liver parenchyma and the almost stable signal intensity in malignant liver tumors (Saini et al., 1987; Clement et al., 1991; Nakayama et al., 1998; Imai et al., 2000; Bourrinet et al., 2006).

To investigate whether this highly stabilized SPIO-alginate is a kind of ideal MR contrast for liver imaging, the pharmacokinetics and tissue distribution of SPIO-alginate in rats were first examined in this study. After that, the efficacy of SPIO-alginate for the detection of liver cancers was evaluated in two kinds of tumor models, VX2 liver tumor in rabbit and primary liver cancer in rat.

2. Materials and methods

2.1. Contrast agent

Typical iron oxide nanoparticles were Fe_3O_4 with a core diameter of 5–10 nm. Meanwhile, SPIO-alginate had a hydrodynamic diameter of 193.8 nm with good stability as well as superparamagnetism, and its ξ-potential was −65.0 mV. T1 and T2 relaxivities of SPIO-alginate in physiological saline (1.5 T, 20 °C) were 7.86 ± 0.20 and $281.2 \pm 26.4\ s^{-1}\ mM^{-1}$, respectively. Other properties of SPIO-alginate were described in detail in the previous publication (Ma et al., 2007, 2007a). For MR imaging experiment, SPIO-alginate was diluted to a concentration of 8.9 μmol Fe/mL with physiological saline.

2.2. Pharmacokinetics, tissue distribution and histological evaluation in normal rats

Male Sprague–Dawley rats weighing 150 ± 20 g were purchased from Experimental Animal Center of Peking University, China. All care and handling of animals were performed with the approval of Institutional Authority for Laboratory Animal Care of Peking University, which followed the guidelines established by the China Council for Animal Care. The animals were anesthetized by intraperitoneal injection of 1.0 g/kg of ethyl carbamate. The pharmacokinetics studies (using whole blood) were carried out with 29 rats which were divided into four groups randomly. The rats were intravenously injected with the following formulations individually: SPIO-alginate at a dose of 109.5 μmol Fe/kg (SPIO-low dose) ($n = 18$), SPIO-alginate at a dose of 218.9 μmol Fe/kg (SPIO-high dose) ($n = 3$), 1 mL 0.6% (w/v) alginate solution (alginate solution) ($n = 3$), and 1 mL physiological saline (saline) ($n = 5$). About 0.3 mL blood samples were taken by retro-orbital venous plexus puncture at 0 min (before intravenous injection), 5 min, 10 min, 30 min, 1 h, 3 h, 6 h, 12 h, 24 h, 48 h, 96 h, 168 h, and 336 h after injection, respectively.

The pharmacokinetics studies (using serum) were obtained in rats by quantitative determination of iron in serum. Twenty rats were divided into four groups ($n = 5$ per group) in random and injected with SPIO-low dose, SPIO-high dose, alginate solution, and saline, respectively. About 0.6 mL blood samples were collected from retro-orbital venous plexus puncture at 0 min, 5 min, 10 min, 30 min, 1 h, 3 h, 6 h, 12 h, and 24 h after injection, respectively. Then each clotted blood sample was centrifuged at 7000 rpm for 20 min to get serum sample.

The basic serum iron concentration was calculated from the average serum iron concentration at 0 min of all the rats. The serum iron concentrations at various time points after administration were calculated by subtracting the basic serum iron concentration. Serum iron concentration–time profiles were analyzed by WinNonlin computer software, Version 3.1 (Pharsight Corporation, Mountain View, CA), using noncompartmental method with bolus intravenously administration. The following parameters were obtained: maximum tissue concentration (C_{max}), elimination rate constant (λ), elimination half-life ($T_{1/2}$), area under the curve (AUC), and mean residence time (MRT).

The tissue distribution of SPIO-alginate at a dose of 109.5 μmol Fe/kg in rats (total 21) were studied at 0, 0.5, 3, 24, 48, 96, and 336 h after injection, which was performed simultaneously with the blood pharmacokinetics study of SPIO-low dose. Tissues of interest (blood, liver, spleen, heart, lungs, and kidneys) were collected immediately at various time points, weighted, and frozen at −20 °C until analysis.

Liver and spleen concentration-time profiles were analyzed by WinNonlin computer software using a noncompartmental method with a single extravascular dosing. The iron concentrations in liver and spleen at various time points were calculated

by subtracting the iron concentration in liver or in spleen at 0 h (before injection), respectively. The following parameters were obtained: time of maximum concentration (T_{max}), C_{max}, λ, $T_{1/2}$, AUC, and MRT.

Liver and spleen were removed at 0.5, 24, 96, and 336 h after injection of SPIO-low dose, and at 336 h after injection of SPIO-high dose and alginate solution, respectively. Then the samples were fixed in 4% paraformaldehyde solution (pH 7.4) for hematoxylin-eosin (HE) staining and Perls staining. The liver and spleen section specimens were examined under a light microscopy after staining.

2.3. Iron content measurement

For quantitative determination of iron content, blood, serum and tissue samples were digested in a beaker with the mixed acid of HNO_3–$HClO_4$ (4:1, v:v) for 48 h at room temperature, and then evaporated to dryness at 100 °C by sand bath with electric hot plate. Finally 37.5% HCl solution was added to the beaker to dissolve the solid and the iron content was determined by *o*-phenanthroline method (Hagar et al., 2003).

2.4. Tumor models of rats and rabbits

Male Sprague–Dawley rats (130–140 g, total 35) were used. The model of primary liver cancer in rats ($n = 29$) was established by giving 70 mg diethylnitrosoamine (DENA, Sigma–Aldrich, USA) per kg weight 14 times at 7-d intervals through intragastric administration with physiological saline. As DENA was sensitive to light, a fresh solution was prepared for each administration and kept in dark bottles for short periods. The rats of control group ($n = 6$) were raised in the normal condition.

VX2 rabbit tumor was cut into small pieces (about 1 mm^3), and then implanted into left hepatic lobe to establish single liver cancer in rabbit. After implantation, VX2 tumor rapidly developed in the liver and the implanted tumor formation was detected by computed tomography (CT) on week 2. The surgery and implantation procedures have been described in detail in the previous publication (Hauff et al., 1997).

2.5. MR imaging in normal rat

All MR imaging examinations were performed by using a clinical 3.0 T MR scanner (Signa Horizon, General Electric Medical Systems, Milwaukee, WI) with a surface coil. For the investigations of liver enhancement in normal rats, the normal rats ($n = 6$) were imaged before and after injection of SPIO-alginate at a dose of 20 μmol Fe/kg through femoral vein. T1-weighted fast spin echo (FSE) or spoiled gradient-recalled (SPGR) sequence, T2-weighted fast recovery fast spin echo (FRFSE) sequence, and T2*-weighted gradient-recalled echo (GRE) sequence were used for the MR imaging. All the sequences were applied with a bandwidth of 31.25 kHz and slice thickness of 3 mm. Other parameters were as follows: T1-weighted FSE sequence (TE 14.6 ms; TR 800 ms; Echo train length 3; Matrix 288 × 192; NEX 4; FOV 8 × 8); T1-weighted SPGR sequence (TE 3.7 ms; TR 100 ms; Flip angles 60°; Matrix 128 × 128; NEX 6; FOV 8 × 4); T2-weighted FRFSE sequence (TE 150 ms; TR 3000 ms; Echo train length 21; Matrix 128 × 128; NEX 6; FOV 8 × 5.6); T2*-weighted GRE sequence (TE 4.7 ms; TR 300 ms; Flip angles 15°; Matrix 128 × 128; NEX 6; FOV 8 × 4).

2.6. MR imaging in tumor animals and histological evaluation

For rabbits with VX2 tumor, unenhanced and enhanced T2*-weighted images were investigated before and after injection of SPIO-alginate at a dose of 20 μmol Fe/kg using SPGR sequence with the following parameters: TR of 220 ms, TE of 5.2 ms, flip angles of 70°, slice thickness of 4 mm, slice gap of 1.0 mm, matrix of 512 × 160, field of view of 13 × 13, and bandwidth of 62.5 kHz.

For rats with primary liver cancer, unenhanced and enhanced images were obtained before and after injection of SPIO-alginate at a dose of 20 μmol Fe/kg using T2*-weighted GRE sequence with the parameters just mentioned above in MR imaging for normal rats. The rats were sacrificed within 2–12 h after MR imaging evaluation. Then, liver specimens were fixed, the size, number, and shape of the lesions were observed, and the lesions were histologically identified after HE staining and Perls staining. The pathological changes e.g. hyperplastic nodules, cirrhotic and HCC, were also observed.

2.7. Imaging analysis

Quantitative analysis was performed by using an operator defined region of interest (ROI) of 6 mm^2 on T1-weighted, T2-weighted and T2*-weighted images, respectively. Major vessels were avoided when the signal intensities of liver parenchyma and tumor were measured. Measurements included signal intensity (SI) of the HCC (SI_{HCC}), the liver parenchyma without cirrhosis (SI_{liver}), the liver parenchyma with cirrhosis ($SI_{cirrhosis}$), and standard deviation of noise ($S.D._{noise}$), respectively. Signal-to-noise ratio (SNR) was then calculated on both pre- and post-SPIO-alginate images by taking the SI_{HCC}, SI_{liver} or $SI_{cirrhosis}$ dividing by each $S.D._{noise}$. In addition, contrast-to-noise ratio (CNR) was calculated with the following formula: $(SI_{HCC} - SI_{cirrhosis})/S.D._{noise}$, and the relative contrast was expressed as $SI_{HCC}/SI_{cirrhosis}$.

3. Results

3.1. Pharmacokinetics of SPIO-alginate in normal rats

After injection of SPIO-alginate at both low dose and high dose, the blood iron concentration first gradually decreased from the maximal concentration at 0.083 h to the lowest concentration at 48 h (from 515.5 to 266.3 μg/mL for SPIO-low dose group, and from 647.7 to 333.6 μg/mL for SPIO-high dose group, respectively), and then recovered to the initial concentration before injection (about 471.9 μg/mL) at 96 h. In addition, the blood iron concentration after injection of alginate solution and saline also showed the similar profile (mildly down and up), and